Inorganic Chemistry

Article

pubs.acs.org/IC

Syntheses, Photoluminescence, and Electroluminescence of a Series of Iridium Complexes with Trifluoromethyl-Substituted 2-Phenylpyridine as the Main Ligands and Tetraphenylimidodiphosphinate as the Ancillary Ligand

Qiu-Lei Xu, Cheng-Cheng Wang, Tian-Yi Li, Ming-Yu Teng, Song Zhang, Yi-Ming Jing, Xu Yang, Wei-Nan Li, Chen Lin, You-Xuan Zheng,* Jing-Lin Zuo, and Xiao-Zeng You

State Key Laboratory of Coordination Chemistry, Nanjing National Laboratory of Microstructures, School of Chemistry and Chemical Engineering, Nanjing University, Nanjing 210093, People's Republic of China

Supporting Information

ABSTRACT: Five bis-cyclometalated iridium complexes with tifluoromethyl-substituted 2-phenylpyridine (ppy) at different positions of its phenyl group as the main ligands and tetraphenylimidodiphosphinate (tpip) as the ancillary ligand, **2**–**6** (**1** is a trifluoromethyl-free complex), were prepared, and their X-ray crystallography, photoluminescence, and electrochemistry were investigated. The number and positions of trifluoromethyl groups at the phenyl ring of ppy greatly affected the emission spectra of Ir^{3+} complexes, and their corresponding emission peaks at 533, 502, 524, 480, and 542 nm were observed at room temperature, respectively. Constructed with complexes **2**–**6** as the emitters, respectively, the organic light-emitting diodes (OLEDs) with the structure of indium–tin oxide/1,1-bis[4-(di-*p*-tolylamino)phenyl]cyclohexane (30 nm)/Ir (*x* wt %):bis[3,5-bis(9*H*-carbazol-9-yl)phenyl]-diphenylsilane (15 nm)/1,3,5-tris(1-phenyl-1*H*-benzo[*d*]imidazol-2-yl)phenyl (45 nm)/LiF (1 nm)/Al (100 nm) showed good performances. Particularly, device G4 based on 4-trifluoromethyl-substituted complex **4** with *x* = 8 wt % obtained a maximum luminance of over 39000 cd m^{-2} and maximum luminance efficiency (η_L) and power efficiency (η_p) of 50.8 cd A^{-1} and 29.0 lm W^{-1}, respectively. The results suggested that all of the complexes **2**–**6** would have potential applications in OLEDs.

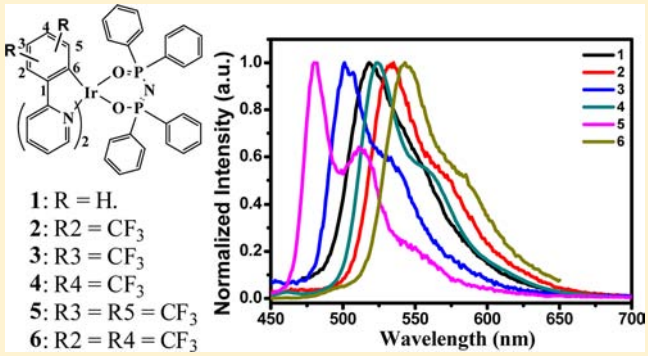

INTRODUCTION

Phosphorescent Ir^{3+} complexes play an important part in efficient organic light-emitting diode (OLED) fabrication because of the high quantum efficiency and short lifetime of triplet excited states.[1] These Ir^{3+} complexes have very strong spin–orbit coupling, which introduces intersystem crossing to mix the singlet and triplet excited states and change the spin-forbidden radiative relaxation from the triplet excited state to be allowed. As a result, both singlet and triplet excitons can be harvested for light emission and the internal quantum efficiency of these Ir^{3+} complexes can achieve 100% theoretically. In particular, phosphorescent materials based on iridium(III) 2-phenylpyridine (ppy) derivatives have drawn much more attention and been successfully applied in OLED fabrication because they are efficient phosphorescent materials emitting lights in the region of red, green, and blue, which can be tuned by modifying the ppy main ligands as well as by introducing diverse ancillary ligands.[2]

Different substituted groups at the different positions of the ppy ring in Ir^{3+} complexes will result in various spectrum character. Ir^{3+} complexes carrying fluorinate ppy ligands were reported with good performances,[3] which suggested that the introduction of electron-withdrawing trifluoromethyl groups improved the OLED performances effectively in several ways:[4] (i) fluorinated compounds can usually be sublimed with ease for thin film deposition; (ii) the bulky CF_3 substituent can affect the molecular packing, providing steric protection around the metal, which can suppress the self-quenching behavior; (iii) fluorination can enhance the electron mobility and result in a better balance of charge injection and transfer. The effect of F atoms on the photophysics of homoleptic complexes was evaluated by various groups. Some groups also studied various heteroleptic fluorinated iridium complexes, which suggested that the fluorine and trifluoromethyl groups in different positions of the ppy ligands showed different effects on the emission properties.[4,5] However, comprehensive and deeper studies are still needed.

Additionally, the emission energy of heteroleptic complexes $[Ir(C^N)_2(LX)]$ can be fine-tuned by a combination of main (C^N) ligands and LX types of ancillary ligands (such as acac = acetylacetone, pic = picolinate, sal = salicylimine, iq =

Received: November 16, 2012
Published: April 15, 2013

   dx.doi.org/10.1021/ic302510p | *Inorg. Chem.* 2013, 52, 4916–4925

isoquinolinecarboxylate, and bpz = pyrazolylborate).[6] Our group has reported highly efficient green and blue-green phosphorescent OLEDs by introducing tetraphenylimidodiphosphinate (tpip) as an ancillary ligand for the first time.[7a] Compared with the acac ligand, tpip has a stronger polar P=O bond, which may improve the electron mobility of the Ir^{3+} complex and benefit its OLED performances,[7] which suggests that tpip is an actually useful ancillary ligand for the phosphorescent Ir^{3+} complex. To investigate the effect of the substituted position and number of the trifluoromethyl substituent on the phenyl group of the ppy ring in the Ir^{3+} complex for its OLED performance and explore the application of tpip ligands, we synthesized a series of Ir^{3+} complexes with tpip as the ancillary ligand and studied their OLED characteristics.

EXPERIMENTAL SECTION

Materials and Measurements. All reagents and chemicals were purchased from commercial sources and used without further purification. ^{1}H NMR spectra were measured on a Bruker AM 400 spectrometer or a Bruker AM 500 spectrometer. Mass spectrometry (MS) spectra were obtained with an electrospray ionization (ESI) mass spectrometer (LCQ Fleet, Thermo Fisher Scientific) or matrix-assisted laser desorption ionization time-of-flight (MALDI-TOF) mass spectrometer (Bruker Daltonic Inc.). Elemental analyses for C, H, and N were performed on an Elementar Vario MICRO analyzer. Absorption and photoluminescence (PL) spectra were measured on a UV-3100 spectrophotometer and a Hitachi F-4600 PL spectrophotometer, respectively. The decay lifetimes were measured with an Edinburgh Instruments FLS920P fluorescence spectrometer in degassed CH_2Cl_2 solution and the solid state at room temperature (RT). Cyclic voltammetry (CV) measurements were conducted on a MPI-A multifunctional electrochemical and chemiluminescent system (Xi'an Remex Analytical Instrument Ltd. Co., China) at RT, with a polished platinum plate as the working electrode, platinum thread as the counter electrode, and Ag-$AgNO_3$ (0.1 M) in CH_2Cl_2 as the reference electrode; *tetra-n*-butylammonium perchlorate (0.1 M) was used as the supporting electrolyte, with Fc^+/Fc as the internal standard, and the scan rate was 0.1 V s^{-1}.

The luminescence quantum efficiencies were calculated by a comparison of the emission intensities (integrated areas) of a standard sample [$Ir(ppy)_3$] and the unknown sample according to eq 1.[8]

$$\Phi_{unk} = \Phi_{std}\left(\frac{I_{unk}}{I_{std}}\right)\left(\frac{A_{std}}{A_{unk}}\right)\left(\frac{\eta_{unk}}{\eta_{std}}\right)^2 \quad (1)$$

where Φ_{unk} and Φ_{std} are the luminescence quantum yields of the unknown sample and $Ir(ppy)_3$, respectively. I_{unk} and I_{std} are the integrated emission intensities of the unknown sample and $Ir(ppy)_3$ solution, respectively. A_{unk} and A_{std} are the absorbances of the unknown sample and $Ir(ppy)_3$ solution at their excitation wavelengths, respectively. The η_{unk} and η_{std} terms represent the refractive indices of the corresponding solvents (pure solvents were assumed). The Φ_{std} value of $Ir(ppy)_3$ has been revalued to be 0.4.[9]

Density functional theory (DFT) calculations using the B3LYP[10a] functional were performed. The basis set used for C, H, N, O, F, and P atoms was 6-31G(d,p),[10b] while the LanL2DZ basis set were employed for Ir atoms.[10c] The solvent effect of CH_2Cl_2 was taken into consideration using the conductor-like polarizable continuum model (C-PCM).[10d] All of these calculations were performed with *Gaussian 09*.[10e]

X-ray Crystallography. The single crystals of complexes were carried out on a Bruker SMART CCD diffractometer using monochromated Mo Kα radiation (λ = 0.71073 Å) at RT. Cell parameters were retrieved using *SMART* software and refined using *SAINT*[11] on all observed reflections. Data were collected using a narrow-frame method with scan widths of 0.30° in ω and an exposure time of 10 s $frame^{-1}$. The highly redundant data sets were reduced using *SAINT* and corrected for Lorentz and polarization effects. Absorption corrections were applied using *SADABS*[12] supplied by Bruker. The structures were solved by direct methods and refined by full-matrix least squares on F^2 using the program *SHELXS-97*.[13a] The positions of the metal atoms and their first coordination spheres were located from direct methods on E-maps; other non-H atoms were found in alternating difference Fourier syntheses and least-squares refinement cycles and, during the final cycles, refined anisotropically. H atoms were placed in calculated positions and refined as riding atoms with a uniform value of U_{iso}.

OLED Fabrication and Measurement. All OLEDs with an emission area of 0.1 cm^2 were fabricated on the prepatterned indium-tin oxide (ITO)-coated glass substrate with a sheet resistance of 15 Ω sq^{-1}. The substrate was cleaned by ultrasonic baths in organic solvents followed by ozone treatment for 20 min. All chemicals used for electroluminescence (EL) devices were sublimed in vacuum (2.2×10^{-4} Pa) prior to use. The 30 nm hole-transporting material of 1,1-bis[4-(di-*p*-tolylamino)phenyl]cyclohexane (TAPC) was first deposited on the ITO glass substrate. The phosphor (*x* wt %) and bis[3,5-di(9*H*-carbazol-9- yl)phenyl]diphenylsilane (SimCP2) host were coevaporated to form a 15 nm emitting layer from two separate sources. Successively, 1,3,5-tri(1-phenyl-1*H*-benzo[*d*]imidazol-2-yl)-phenyl (TPBi; 45 nm), LiF (1 nm), and Al (100 nm) were evaporated. The vacuum was less than 1×10^{-5} Pa during all material deposition. The current density−voltage−luminance (*J*−*V*−*L*) characteristics and current efficiency versus *J* curves of the devices were measured with a computer-controlled Keithley 2400 source meter with a calibrated silicon diode in air without device encapsulation. The EL spectra were measured with a Hitachi F-4600 PL spectrophotometer. On the basis of the uncorrected PL and EL spectra, the Commission Internationale de l'Eclairage (CIE) coordinates were calculated using a test program of the Spectra scan PR650 spectrophotometer.

Syntheses. *General Syntheses of Ligands.* The synthesis procedures of ligands are listed in Scheme 1. Tetraphenylimidodiphosphinate acid (Htpip) and potassium tetraphenylimidodiphosphinate (Ktpip) were prepared according to the literature.[7,14] All CF_3-substituted ligands **L2**−**L6** with a ppy core were synthesized by the reaction of the corresponding 2-bromopyridine (21.1 mmol) and arylboronic acids (25.5 mmol) using tetrakis(triphenylphosphine)-palladium(0) (0.63 mmol) as the catalyst in 50 mL of tetrahydrofuran.

Scheme 1. Synthetic Routes of Ligands and Complexes

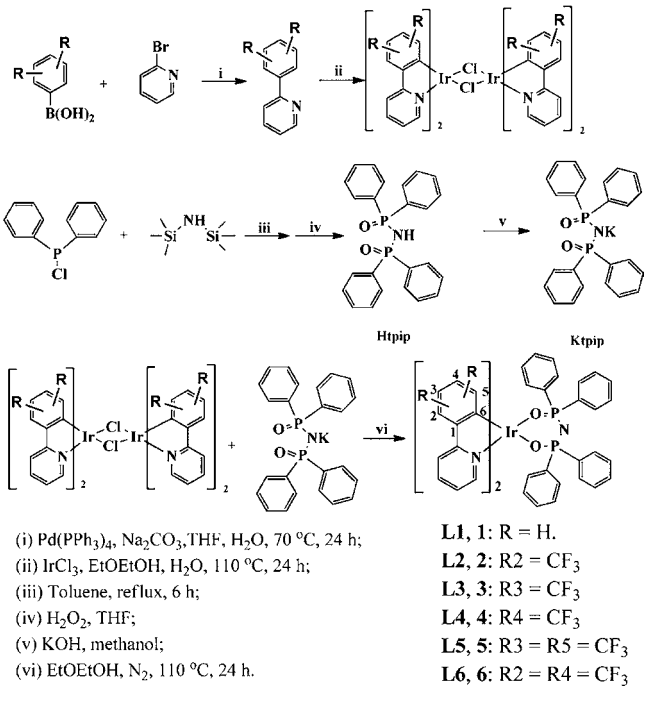

dx.doi.org/10.1021/ic302510p | Inorg. Chem. 2013, 52, 4916−4925

Table 1. Crystallographic Data and Structure Refinement for Complexes 1−3, 5, and 6

	1	2	3	5	6
formula	$C_{46}H_{36}IrN_3O_2P_2$	$C_{48}H_{34}F_6$ $IrN_3O_2P_2$	$C_{288}H_{206}F_{36}$ $Ir_6N_{18}O_{13}P_{12}$	$C_{50}H_{32}F_{12}IrN_3O_2P_2$	$C_{50}H_{32}F_{12}IrN_3O_2P_2$
fw	916.92	1052.92	6335.55	1188.93	1188.93
T (K)	296(2)	296(2)	291(2)	293(2) K	296(2) K
wavelength (Å)	0.71073	0.71073	0.71073	0.71073	0.71073
cryst syst	monoclinic	monoclinic	monoclinic	triclinic	monoclinic
space group	$P2_1/c$	$P2_1/c$	$C2/c$	$P\bar{1}$	$P2_1/c$
a (Å)	15.5459(9)	9.7148(14)	41.6691(12)	10.7141(3)	10.9585(5)
b (Å)	11.1607(7)	20.775(3)	15.2305(7)	11.7373(4)	17.7561(9)
c (Å)	23.5153(13)	20.991(3)	23.3920(10)	18.7457(6)	24.2144(12)
α (deg)	90	90	90	79.9040(10)	90
β (deg)	106.3910	102.074(2)	113.056(2)	84.4300(10)	93.6330
γ (deg)	90	90	90	87.9820(10)	90
V (Å^3)	7295(2)	4256.5(5)	13659.7(9)	2309.50(13)	4702.2(4)
Z	4	4	2	2	4
ρ_{calcd} (g cm^{-3})	1.556	1.688	1.540	1.710	1.679
μ(Mo Kα) (mm^{-1})	3.535	3.372	3.069	3.053	2.999
F (000)	1824	2080	6260	1168	2336
range of transm factors (deg)	1.81−26.00	1.96−26.00	1.44−26.00	1.76−25.00	1.69−26.00
reflns collected	23203	24808	41301	13129	28259
unique reflns	7687	8134	13432	8108	9225
GOF on F^2	0.956	1.036	1.018	1.080	1.008
R1,[a] wR2[b] [$I > 2\sigma(I)$]	0.0323, 0.0632	0.0235, 0.0521	0.0478, 0.0998	0.0555, 0.1490	0.0455, 0.1413
R1,[a] wR2[b] (all data)	0.0541, 0.0682	0.0289, 0.0534	0.0693, 0.1049	0.0571, 0.1505	0.05080, 0.1458
CCDC	902470	902471	902472	902474	902473

[a] $R1 = \sum||F_o| - |F_c||/\sum|F_o|$. [b] $wR2 = [\sum w(F_o^2 - F_c^2)^2/\sum w(F_o^2)^2)]^{1/2}$.

After 30 mL of aqueous 2 N Na_2CO_3 was delivered, the reaction mixture was heated at 70 °C for 1 day. The cooled mixture was poured into water, extracted with CH_2Cl_2 (50 mL × 3), and then dried over anhydrous magnesium sulfate. Finally, silica column purification (*n*-hexane:EtOAc = 7:1 as the eluant) gave white solid products.

*2-[2-(Trifluoromethyl)phenyl]pyridine (**L2**).* Yield: 80%. ^{1}H NMR ($CDCl_3$, 400 MHz): δ 7.2−7.6 (m, 4H), 7.49 (d, J = 7.2 Hz, 1H), 7.55 (d, J = 7.3 Hz, 1H), 7.65−7.8 (m, 1H), 8.60 (m, 1H). MS (ESI): m/z 223 [M$^+$].

*2-[3-(Trifluoromethyl)phenyl]pyridine (**L3**).* Yield: 75%. ^{1}H NMR ($CDCl_3$, 400 MHz): δ 7.1 (m, 1H), 7.44 (t, J = 7.8 Hz, 1H), 7.59−7.71 (m, 3H), 8.06 (d, J = 7.8 Hz, 1H), 8.3 (s, 1H), 8.62 (dd, J = 4.7 and 0.9 Hz, 1H). MS (ESI): m/z 223 [M$^+$].

*2-[4-(Trifluoromethyl)phenyl]pyridine (**L4**).* Yield: 76%. ^{1}H NMR ($CDCl_3$, 400 MHz,): δ 7.1 (ddd, J = 8.6, 4.7, and 2.1 Hz, 1H), 7.55 (d, J = 7.5 Hz, 4H), 7.93 (d, J = 8 Hz, 2H), 8.56 (d, J = 4.4 Hz, 1H). MS (ESI): m/z 223 [M$^+$].

*2-[3,5-Bis(trifluoromethyl)phenyl]pyridine (**L5**).* Yield: 70%. ^{1}H NMR ($CDCl_3$, 400 MHz): δ 8.73 (d, J = 8 Hz, 1H), 8.47 (s, 2H), 7.90 (s, 1H), 7.81 (dd, J = 8 and 2 Hz, 2H), 7.33 (dd, J = 8 and 2 Hz, 1H). MS (ESI): m/z 292 [M$^+$].

*2-[2,4-Bis(trifluoromethyl)phenyl]pyridine (**L6**).* Yield: 80%. ^{1}H NMR ($CDCl_3$, 400 MHz): δ 8.71 (d, aromatic, J = 8 Hz, 1H), 8.02 (s, 1H), 7.88 (d, J = 8 Hz, 1H), 7.79 (dd, J = 8 and 2 Hz, 1H), 7.66 (d, J = 8 Hz, 1H), 7.44 (d, J = 8 Hz, 1H), 7.37 (dd, J = 8 and 2 Hz, 1H). MS (ESI): m/z 292 [M$^+$].

General Syntheses of Complexes. The synthesis of complex **4** was reported in our group,[7] and complexes **1**−**3**, **5**, and **6** were synthesized according to similar procedures.[7,15] A mixture of $IrCl_3{\cdot}3H_2O$ (1 mmol) and **L** (2.5 mmol) in 2-ethoxyethanol and water (20 mL, 3:1, v/v) was refluxed for 24 h. After cooling, the yellow solid precipitate was filtered to give the crude cyclometalated Ir^{3+} chloro-bridged dimer. Then a slurry of the crude chloro-bridged dimer (0.2 mmol) and Ktpip (0.5 mmol) in 2-ethoxyethanol (20 mL) was refluxed for 24 h. After the mixture was cooled to RT, the solvent was evaporated at low pressure. The crude product was washed by water and then chromatographed using CH_2Cl_2 to give complexes **1**−**6**, which were further purified again by sublimation in vacuum.

*Complex **1**.* Yield: 40%. ^{1}H NMR (500 MHz, $CDCl_3$): δ 9.08 (d, J = 5.4 Hz, 2H), 7.78 (dd, J = 12.3 and 6.5 Hz, 4H), 7.68 (d, J = 8.1 Hz, 2H), 7.55 (d, J = 7.5 Hz, 2H), 7.46−7.30 (m, 12H), 7.16 (t, J = 7.4 Hz, 2H), 6.99 (td, J = 7.6 and 2.9 Hz, 4H), 6.83 (t, J = 7.3 Hz, 2H), 6.68 (t, J = 7.9 Hz, 2H), 6.61 (t, J = 7.0 Hz, 2H), 6.17 (d, J = 7.6 Hz, 2H). MALDI-TOF (M$^+$): 918. Anal. Calcd for $C_{46}H_{36}IrN_3O_2P_2$: C, 60.25; H, 3.96; N, 4.58. Found: C, 60.47; H, 4.07; N, 4.49.

*Complex **2**.* Yield: 60%. ^{1}H NMR (500 MHz, $CDCl_3$): δ 9.17 (d, J = 5.6 Hz, 2H), 8.18 (d, J = 8.5 Hz, 2H), 7.83−7.67 (m, 4H), 7.51−7.30 (m, 12H), 7.26 (d, J = 7.5 Hz, 2H), 7.17 (t, J = 8.0 Hz, 2H), 7.01 (td, J = 7.6 and 3.0 Hz, 4H), 6.67 (t, J = 7.7 Hz, 2H), 6.61 (t, J = 7.0 Hz, 2H), 6.21 (d, J = 7.6 Hz, 2H). MALDI-TOF (M$^+$): 1054. Anal. Calcd for $C_{48}H_{34}F_6IrN_3O_2P_2$: C, 54.75; H, 3.25; N, 3.99. Found: C, 54.94; H, 3.32; N, 4.01.

*Complex **3**.* Yield: 55% ^{1}H NMR (500 MHz, $CDCl_3$): δ 9.06 (d, J = 5.1 Hz, 2H), 7.77 (dd, J = 17.4 and 8.7 Hz, 8H), 7.51 (td, J = 8.0 and 1.4 Hz, 2H), 7.43−7.30 (m, 10H), 7.17 (t, J = 8.0 Hz, 2H), 7.00 (td, J = 7.7 and 3.0 Hz, 4H), 6.88 (d, J = 9.2 Hz, 2H), 6.70 (t, J = 7.1 Hz, 2H), 6.24 (d, J = 8.1 Hz, 2H). MALDI-TOF (M$^+$): 1054. Anal. Calcd for $C_{48}H_{34}F_6IrN_3O_2P_2$: C, 54.75; H, 3.25; N, 3.99. Found: C, 54.70; H, 3.28; N, 4.01.

*Complex **4**.* Yield: 70%. ^{1}H NMR (500 MHz, DMSO): δ 8.92 (d, J = 5.5 Hz, 1H), 8.19 (d, J = 8.1 Hz, 1H), 7.95 (d, J = 8.1 Hz, 1H), 7.77 (t, J = 7.8 Hz, 1H), 7.66 (dd, J = 11.7 and 7.3 Hz, 2H), 7.48−7.36 (m, 3H), 7.27−7.14 (m, 3H), 7.11 (d, J = 8.0 Hz, 1H), 7.02 (dt, J = 12.9 and 6.2 Hz, 3H), 6.11 (s, 1H). MALDI-TOF (M$^+$): 1054. Anal. Calcd for $C_{48}H_{34}F_6IrN_3O_2P_2$: C, 54.75; H, 3.25; N, 3.99. Found: C, 54.68; H, 3.16; N, 4.07.

*Complex **5**.* Yield: 68%. ^{1}H NMR (500 MHz, $CDCl_3$): δ 8.81 (d, J = 5.6 Hz, 2H), 8.01 (s, 2H), 7.74−7.57 (m, 6H), 7.50 (s, 2H), 7.40−7.27 (m, 8H), 7.24 (dd, J = 12.6 and 7.4 Hz, 6H), 7.10 (td, J = 7.4 and 3.0 Hz, 4H), 6.49 (t, J = 6.6 Hz, 2H). MALDI-TOF (M$^+$): 1188. Anal. Calcd for $C_{50}H_{32}F_{12}IrN_3O_2P_2$: C, 50.51; H, 2.71; N, 3.53. Found: C, 50.20; H, 2.60; N, 3.51.

*Complex **6** .* Yield: 72%. ^{1}H NMR (500 MHz, $CDCl_3$): δ 9.13 (s, 2H), 8.24 (d, J = 8.2 Hz, 2H), 7.76 (d, J = 8.2 Hz, 4H), 7.54 (d, J = 26.4 Hz, 4H), 7.39 (s, 10H), 7.18 (s, 2H), 7.02 (s, 4H), 6.74 (s, 2H), 6.32 (s, 2H). MALDI-TOF (M$^+$): 1188. Anal. Calcd for

dx.doi.org/10.1021/ic302510p | Inorg. Chem. 2013, 52, 4916−4925

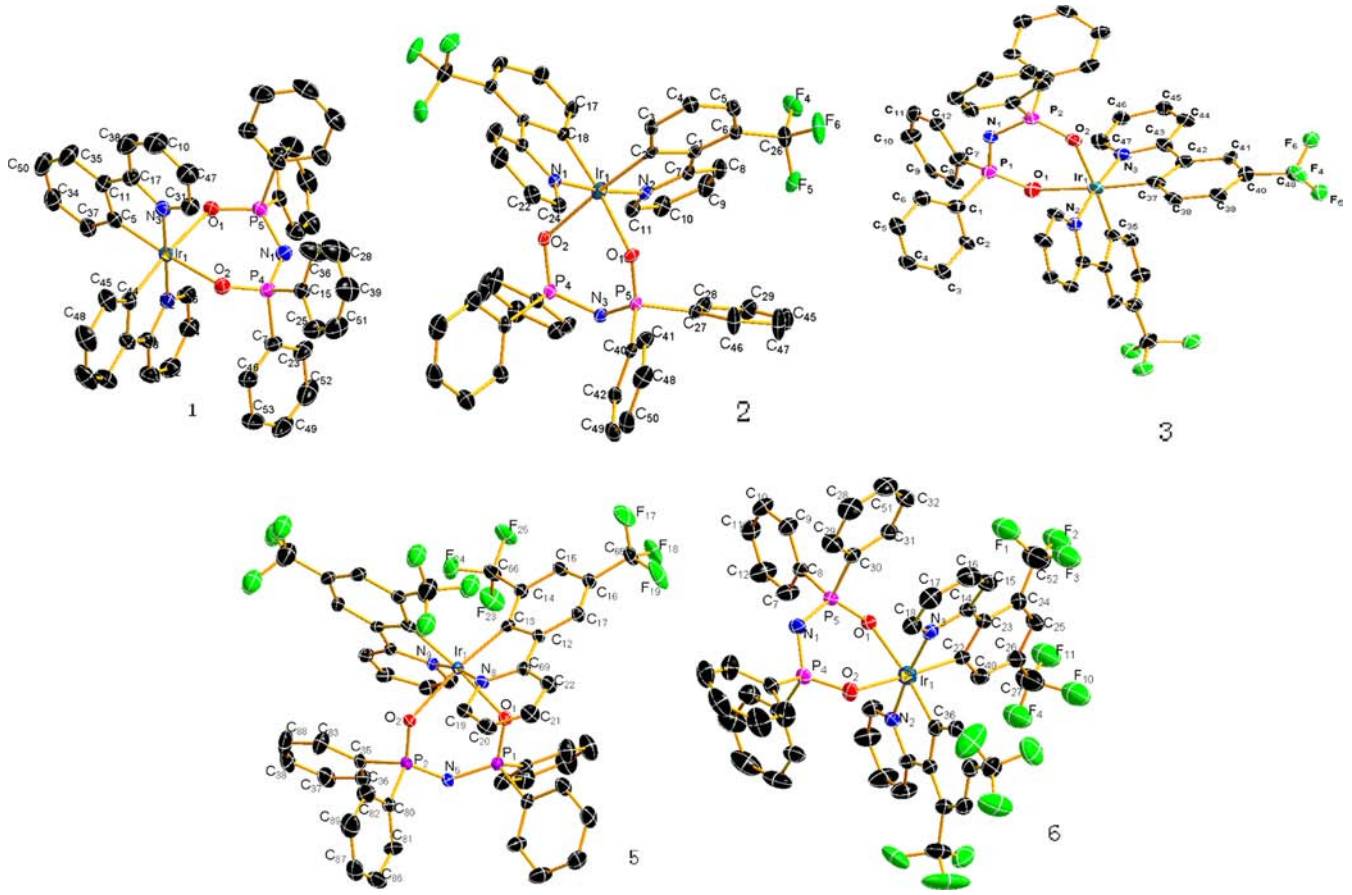

Figure 1. ORTEP diagrams of complexes **1**−**3**, **5**, and **6** with atom-numbering schemes. H atoms are omitted for clarity. Ellipsoids are drawn at the 30% probability level.

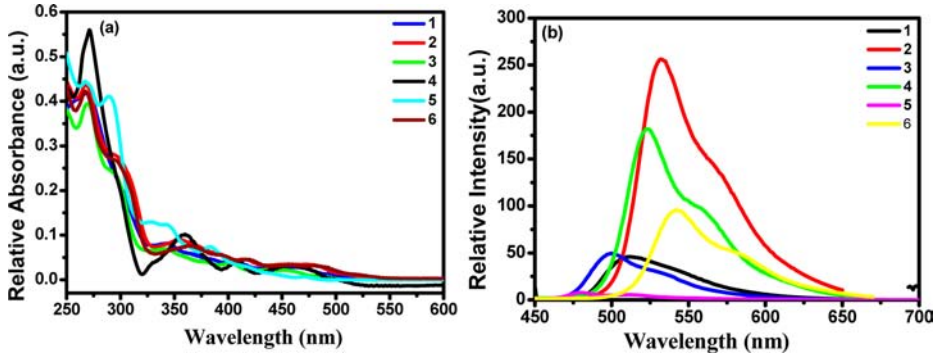

Figure 2. Absorption (a) and relative emission (b) spectra of complexes **1**−**6** in degassed dichloromethane (2×10^{-5} M) at RT.

$C_{50}H_{32}F_{12}IrN_3O_2P_2$: C, 50.51; H, 2.71; N, 3.53. Found: C, 50.39; H, 2.68; N, 3.53.

RESULTS AND DISCUSSION

X-ray Crystallography. All single crystals of the five complexes **1**−**3**, **5**, and **6** were grown from sublimation and characterized by X-ray crystallography. Selected parameters of the molecular structures and tables of atomic coordinates are collected in Table 1, and bond lengths and bond angles for each complex are given in the Supporting Information (Tables S1−S5). Figure 1 shows the Oak Ridge thermal ellipsoidal plot (ORTEP)[13b] diagrams given by X-ray analysis of the five complexes. It should be noted that the sterically crowded ligands result in large deformation with regard to the phenyl rings in the complexes. The deformation is caused by steric hindrance originating from repulsion between the trifluoromethyl group located on the phenyl rings and pyridine. The X-ray data show large dihedral angles for complexes **2** [$C_8-C_7-C_1-C_6$, $-13.4(5)°$] and **6** [$C_{15}-C_{14}-C_{23}-C_{24}$, $-11.6(1)°$], which suggests that the CF_3 group in position 2 (close to the pyridine ring) will cause larger molecular deformation. For complex **1** without the CF_3 group, the dihedral angle [$N_3-C_{17}-C_{11}-C_5$] between two rings is only $-0.3(6)$ °, indicating that the two pyridine rings are almost coplanar.

The Ir−N bond lengths observed ranging from 2.017(5) to 2.039(4) Å are similar to values reported for heteroleptic complexes. The average Ir−C [2.006(0) Å] bond length for

dx.doi.org/10.1021/ic302510p | Inorg. Chem. 2013, 52, 4916−4925

Table 2. Photophysical Data of Ir^{3+} Complexes in the CH_2Cl_2 Solution

			emission (λ_{max}, nm)			lifetime (μs)			
complex	T_m/T_d[a] (°C)	absorption [λ, nm (ε, $\times10^3$ M^{-1} cm^{-1})]	298 K (L/S)[b]	77 K	Φ_{em}(%)	τ_L[b]	τ_S[b]	E_{ox} (eV)	HOMO/LUMO[c] (eV)
1	348/381	269 (41.9), 345 (8.7), 408 (4.2), 465 (3.5)	517/541	506	7.1	1.77	1.90	0.76	−5.39/−2.9
2	320/375	268 (43.1), 299 (27.2), 356 (9.1), 418 (4.2)	533/567	518	25.1	2.26	2.12	0.98	−5.61/−3.18
3	311/344	268 (39.3), 293 (24.2), 342 (7.1), 454 (2.3)	502/514	494	7.0	2.14	1.85	1.04	−5.78/−3.25
4	327/361	270 (55.4), 359 (10.2), 408 (4.1), 458 (3.4)	524/564	521	23.3	1.86	2.28	0.99	−5.44/−2.98
5	334/358	267 (44.7), 288 (41.0), 342 (12.4), 383 (7.2)	480/487	484	0.88	1.83	2.69	1.26	−5.92/−3.29
6	266/361	267 (42.6), 297 (27.2), 365 (7.1), 418 (4.3)	542/548	536	11.0	3.61	3.88	1.16	−5.82/−3.46

[a] T_m: melting temperature. T_d: decomposed temperature. [b] L: liquid. S: solid. [c] HOMO/LUMO means that the value was calculated from experimental data.

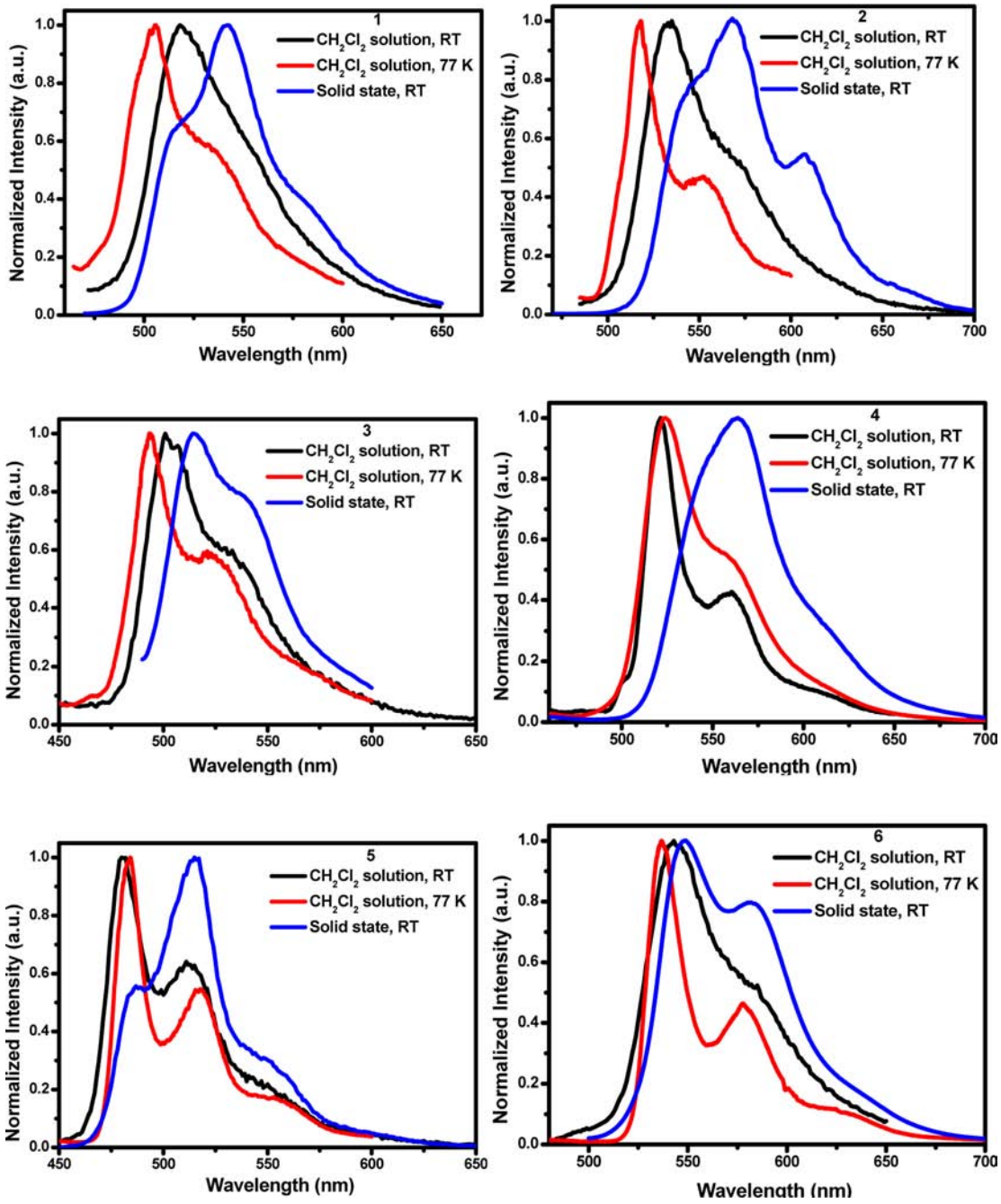

Figure 3. Normalized emission spectra of complexes **1**−**6** in the CH_2Cl_2 solution at RT and 77 K and in the solid state.

complex **5** is slightly longer than that of other complexes [Ir−C 1.980(1) Å], which is most likely due to the electron-withdrawing CF_3 group in position 3, resulting in weaker adjacent Ir−C bonding and stronger corresponding Ir−O

dx.doi.org/10.1021/ic302510p | Inorg. Chem. 2013, 52, 4916−4925

bonding. Furthermore, the C−C and C−N bond lengths and angles are within normal ranges and are in agreement with the corresponding parameters described in other similarly constituted complexes.[16]

Electronic Spectroscopy. The UV−vis absorption spectra of complexes **1**−**6** in CH_2Cl_2 at 2×10^{-5} M are shown in Figure 2a, and the electronic absorption data are listed in Table 2. The absorption of these complexes shows intense bands with extinction coefficients on the order of 10^4 M^{-1} cm^{-1} below 320 nm, which were assigned to the spin-allowed intraligand $^1LC(^3\pi\rightarrow\pi^*)$ transition of cyclometalated ppy derivatives and tpip ligands. The band around 400 nm can be assigned to spin-allowed metal−ligand charge-transfer (^{1}MLCT) bands with extinction coefficients on the order of 10^3 M^{-1} cm^{-1}. The spin-forbidden ^{3}MLCT transition bands around 450 nm indicate an efficient spin−orbit coupling that is prerequisite for phosphorescent emission.

Compared with complex **1** in CH_2Cl_2 with a weak emission band at 517 nm at RT, complexes **2**, **4**, and **6** show much stronger red-shifted emission at 533, 524, and 542 nm, whereas **3** and **5** are blue-shifted to 502 and 480 nm, respectively (Figure 2b). Especially, complex **5** exhibits the weakest PL intensity and lowest quantum yield (0.88%). The results suggest that the position and number of the trifluoromethyl group on the phenyl ring affect the emitting properties of Ir^{3+} complexes. The trifluoromethyl group on position 3 shows a hypsochromic shift of the emission of the complex, and the trifluoromethyl group on positions 2 and 4 shows a bathochromic shift of the emission of the complex. Additionally, complex **2** has a stronger bathochromic effect and a higher quantum yield than those of complex **4**. Compared to the unsubstituted complex **1**, in the case of complex **5**, where CF_3 groups are in positions 3 and 5, there is a strong hypsochromic effect (λ_{max} = 480 nm), indicating that those positions and numbers of CF_3 groups are the most effective in tuning the emission toward the blue region. Conversely, in comparison with complex **1**, complex **6** with two CF_3 groups in the meta position of the coordinating C shows a bathochromic shift in the emission maximum of 25 nm (892 cm^{-1}). This behavior is consistent with the inductive-only nature of the CF_3 group, which renders the meta positions the less electron deficient on the aromatic ring.[5b]

According to the previous work,[17] phosphorescence spectra from the $LC(^3\pi\rightarrow\pi^*)$ state display vibronic progressions, while those from the ^{3}MLCT state are broad and featureless. Figure 3 shows the phosphorescence spectra of the Ir^{3+} complexes measured at RT (in solution and in the solid state) and at 77 K. Compared with $Ir(ppy)_3$, which was assumed to be essentially dominated by the excited triplet energy of ppy-centered ^{3}MLCT, we conclude that complexes **1**−**6** gain larger contributions from the MLCT state and the lowest excited states are likely to dominate the ^{3}MLCT excited state.

As shown in Figure 3, the phosphorescence spectra of the Ir^{3+} complexes suffer the rigidochromic effect: the phosphorescence bands shift to blue on going from RT to 77 K. The rigidochromic effect on some kinds of transition-metal complexes has been previously reported.[18] Because of the low viscosity of the medium at RT, solvent molecules in the vicinity of the excited-state molecule readily undergo reorientation by the dipole−dipole interaction within the lifetime of the excited state, resulting in the formation of a fully relaxed excited state. Thus, the emission at RT occurs from a fully relaxed excited state. On the other hand, the excited state at 77 K emits before solvent relaxation occurs, resulting in rigidochromic effects on the emission spectra. Among them, complexes **1**−**3** and **6** show obvious blue shift, while complex **4** shifts very slightly [only 3 nm (110 cm^{-1})]. The most surprising result is that complex **5** even shows some slight red shifting. As we know, the phosphorescence lifetime (τ_p) is the crucial factor that determines the rate of triplet−triplet annihilation in the OLEDs. A longer τ_p of the material usually causes more severe triplet−triplet annihilation.[19] The lifetimes of complexes **1**−**6** are in the range of microseconds in the CH_2Cl_2 solution (1.77−3.61 μs) and in the solid state (1.85−3.88 μs) at RT (Table 2 and Figures S1−S12 in the Supporting Information), which are indicative of the phosphorescent origin for the excited states in each case.

For most known Ir^{3+} complexes, their emission in the solid state is very weak because of serious triplet−triplet annihilation, but they show efficient light in solution, although there is a solvent effect. However, for complexes **5** and **6**, bright luminescence in the solid state under UV excitation can be observed and their emissions in solution are relatively weak, especially for **5**. This phenomenon, showing weak phosphorescence in solution and enhanced phosphorescence emission in the solid state (EPESS), also called "aggregation-induced phosphorescent emission", has been reported in the literature.[20] In the CH_3CN/H_2O (1:5, v/v) solution, efficient PL can be observed for complexes **5** and **6** (Figure 4), which should originate from molecular microaggregates and is almost 20 times stronger than that in pure CH_3CN.

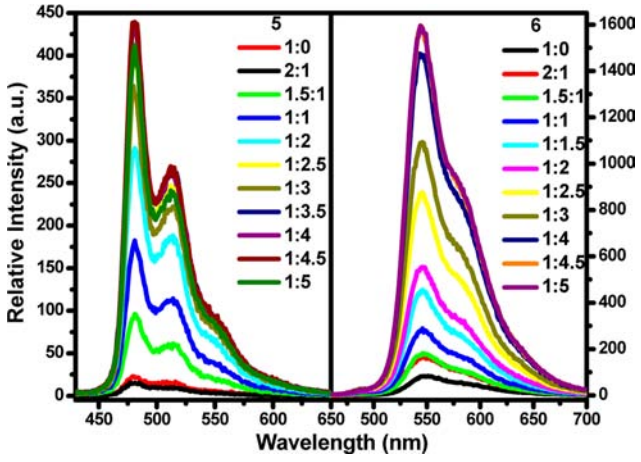

Figure 4. PL spectra of complexes **5** and **6** in the CH_3CN/H_2O solution in different v/v ratios with a concentration of 5.0×10^{-4} mol L^{-1}.

Electrochemistry. To investigate the electronic effects caused by trifluoromethyl substituents on the pyridine rings, CV experiments of complexes **1**−**6** were carried out using ferrocene as the internal standard (Figure 5). The highest occupied molecular orbital (HOMO)/lowest unoccupied molecular orbital (LUMO) energy levels are listed in Table 2. During the anodic scan in CH_2Cl_2, each of the Ir^{3+} complexes exhibits a reversible oxidation with the redox potential in the regions of 0.76 and 1.26 V; this positive oxidation potential is attributed to the metal-centered Ir^{3+}/Ir^{4+} oxidation couple, in accordance with the reported cyclometalated Ir^{3+} systems.[21] A reversible oxidation is observed for complex **1** at 0.76 V. It is noteworthy that complexes **2**−**4** show higher oxidation potentials than that of **1**, which can be ascribed to the great

dx.doi.org/10.1021/ic302510p | Inorg. Chem. 2013, 52, 4916−4925

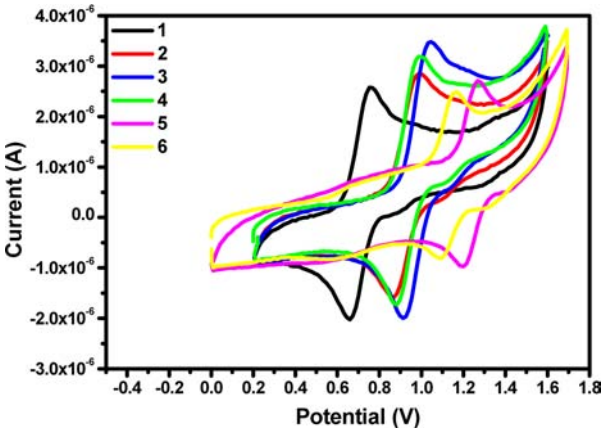

Figure 5. Cyclic voltammograms of complexes **1**–**6**.

electron-withdrawing ability of the trifluoromethyl substituent on the phenyl rings of ppy, making the loss of electrons in complexes more difficult. Therefore, the two trifluoromethyl groups contained in complexes **5** and **6** show even higher oxidation potentials. The HOMO levels of the complexes were calculated from the oxidation potentials and the LUMO levels were calculated from the HOMO and band gap obtained from UV–vis spectra.[22] From Table 2, it can be observed that both the HOMO and LUMO energy levels have been lowered by introduction of the CF_3 group, and complexes **5** and **6** have the lowest values.

Theoretical Calculations. DFT calculations for complexes **1**–**6** were carried out using the *Gaussian 09* computer program to study the orbital distribution employing B3LYP with 6-31G(d,p) basis sets. The effect of substitution on the relative energies of HOMO and LUMO and its impact on the orbital distribution are summarized in Figure 6 and Table S6 in the

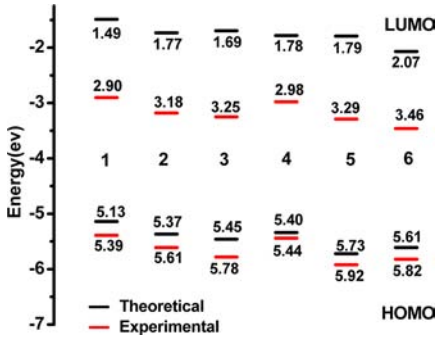

Figure 6. Theoretical (black) and experimental (red, determined by CV) HOMO and LUMO energy levels of complexes **1**–**6**.

Supporting Information, and selected molecular orbitals (MOs) for complexes **1**, **2**, and **6** are shown in Figure 7. For all of the complexes, the HOMO corresponds to a mixture of phenyl groups attached to the pyridyl ring and Ir d orbitals with minor contribution from the tpip ligand, while the LUMO was mainly localized on the ppy ligand with minor contributions from Ir d orbitals and the tpip ligand. Therefore, modification of the phenyl ring changes both the HOMO and LUMO energy. The incorporation of an electron-withdrawing CF_3 group results in a net increase in the HOMO–LUMO gap, resulting from stabilization of both frontier MOs. The trends of the calculated HOMO and LUMO energies of **1**–**6** are basically in agreement with the trends of the measured oxidation and reduction

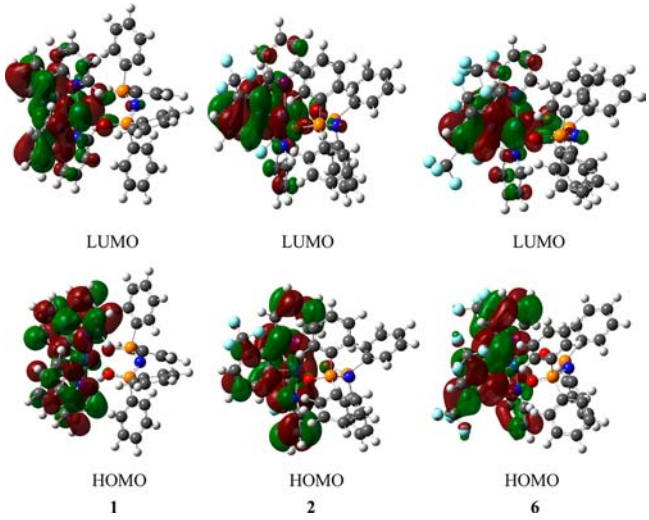

Figure 7. Selected MOs for complexes **1**, **2**, and **6**.

potentials: the lower (more negative) E_{HOMO} and E_{LUMO} energies correspond to the higher (more positive) E_{ox} and E_{red} potentials, respectively. At the same time, the larger calculated HOMO–LUMO energy gap corresponds to a larger electrochemical gap.

Thermal Properties. To investigate the thermal stability of complexes **1**–**6**, thermogravimetric analysis (TGA) and differential scanning calorimetry (DSC) were conducted. If a complex is suitable for application in OLEDs, the decomposition temperature (T_d) should be high enough to guarantee that the complex could be deposited onto the solid face without any decomposition under reduced pressure by sublimation. As shown in Figures S13–S18 in the Supporting Information, the TGA curves of complexes **1**–**6** exhibit good thermal stability up to 380 °C. For complex **1**, no loss of weight was observed up to 350 °C, while the decomposition temperature, which is defined as a 5 wt % loss of weight, appeared at 389 °C. Furthermore, it can be vacuum-evaporated at 280 °C without any decomposition. The introduction of a trifluoromethyl group into the Ir^{3+} complexes will reduce their melting point (T_m) and decomposition temperature to a certain extent. Correspondingly, complexes **2**–**6** are much easier to vacuum-evaporate at lower temperature, 250 °C for **2**–**5**, and 210 °C for **6** at a vacuum of 2.2×10^{-4} Pa, which suggests that all of the complexes have good film-forming ability and make purification by sublimation available.

OLED Performances. To evaluate the EL performances, the OLEDs named G2–G6 using Ir^{3+} complexes **2**–**6** as the emitters were fabricated and investigated with the structure of ITO/TAPC (30 nm)/Ir complexes (*x* wt %):SimCP2 (15 nm)/TPBi (45 nm)/LiF (1 nm)/Al (100 nm). TAPC and SimCP2 were employed as the hole-transporting layer and bipolar host material, respectively. TPBi was used as an electron-transporting and hole-blocking layer. The optimized Ir^{3+} complexes with 8 wt % doped concentration in SimCP2 was used as the emitting layer for G2–G4 and G6, but for G5, the best doped concentration was 20 wt %. Scheme 2 shows the energy diagram of the devices, as well as the molecular structures of the materials used.

The EL spectra, power efficiency, and current efficiency versus *J* curves and voltage–luminance (*V*–*L*) characteristics of each device are shown in Figure 8, and the key EL data are summarized in Table 3. For all of the devices, typical emission

dx.doi.org/10.1021/ic302510p | *Inorg. Chem.* 2013, 52, 4916–4925

Scheme 2. Energy Level Diagram of the HOMO and LUMO Levels (Relative to the Vacuum Level) for Materials Investigated in This Work and Their Molecular Structures

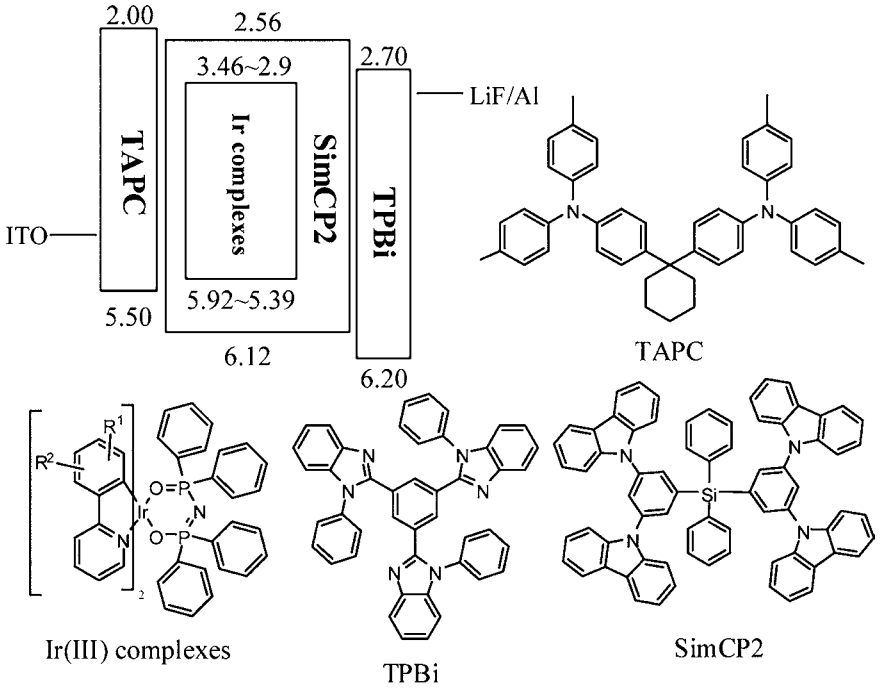

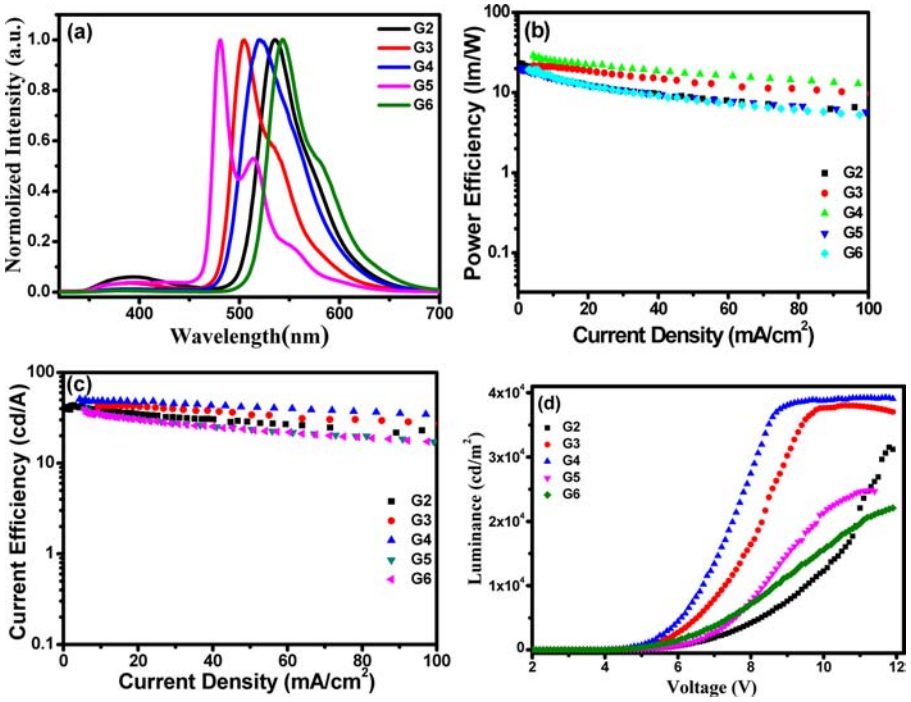

Figure 8. Characteristics of devices with configuration ITO/TAPC (30 nm)/**2**−**6**:SimCP2 (15 nm, *x* wt %)/TPBi (45 nm)/LiF (1 nm)/Al (100 nm) (*x* is 20 wt % for device G5 and 8 wt % for the others): (a) EL spectra at different current densities; (b) power efficiency (η_p) as a function of the current density (*J*); (c) current efficiency (η_c) as a function of the current density (*J*); (d) luminance versus voltage (*L*−*V*) for G2−G6.

maxima of the complexes **2**−**6** at 534, 503, 521, 480, and 543 nm, respectively, are shown at different current densities, suggesting that the energy can be transferred from SimCP2 to the emitter. However, it is noted that there is a little residual emission from the host SimCP2 for each device, which means that the energy and/or charge transfer from the host exciton to the phosphor is not complete upon electrical excitation. The CIE color coordinates are $x = 0.34$, $y = 0.60$ for G2, $x = 0.23$, $y = 0.61$ for G3, $x = 0.17$, $y = 0.41$ for G5, and $x = 0.39$, $y = 0.58$ for G6 at 100 mA cm^{-2}.

All devices display good performances. The turn-on voltages ($V_{turn\text{-}on}$) for devices G2−G6 are 3.5−3.9 V. The maximum luminance efficiency (η_L) and power efficiency (η_p) for device G2 are 43.5 cd A^{-1} and 23.08 lm W^{-1}, respectively, with a maximum luminance of over 31522 cd m^{-2} at a driving voltage of 11.8 V. The driving voltages to reach the practical brightness

dx.doi.org/10.1021/ic302510p | *Inorg. Chem.* 2013, 52, 4916−4925

Table 3. EL Performances of the Devices G2 (x = 8 wt %), G3 (8 wt %), G4 (8 wt %), G5 (x = 20 wt %), and G6 (x = 8 wt %)

device	$V_{turn\text{-}on}$[a] (V)	L_{max}[b] (cd m^{-2}), voltage (V)	$\eta_{p,max}$[c] (lm W^{-1}), voltage (V)	$\eta_{c,max}$[d] (cd A^{-1}), voltage (V)	$\eta_{c,100}$[e]/$\eta_{c,1000}$[f] (cd A^{-1})	L_{100}[g] (cd m^{-2})	CIE[h] (x, y)
G2	3.5	38115, 13.3	23.08, 5.1	43.5, 6.5	33.1/42.4	23604	(0.34, 0.60)
G3	3.6	38005, 10.6	21.16, 6.4	43.13, 6.4	11.3/35.7	27417	(0.23, 0.61)
G4	3.9	39286, 11.7	29.01, 5.6	50.8, 5.5	21.7/43.0	35130	(0.29, 0.63)
G5	3.7	24863, 11.3	20.58, 5.4	39.67, 6.8	27.4/37.6	18228	(0.17, 0.41)
G6	3.6	23411, 14.2	19.60, 6.0	38.68, 6.3	15.5/34.8	17348	(0.39, 0.58)

[a] $V_{turn\text{-}on}$: turn-on voltage recorded at a brightness of 1 cd m^{-2}. [b] L_{max}: maximum luminance. [c] η_p: power efficiency. [d] η_c: current efficiency. [e] $\eta_{c,100}$: current efficiency at the brightness of 100 cd m^{-2}. [f] $\eta_{c,1000}$: current efficiency at the brightness of 1000 cd m^{-2}. [g] L_{100}: luminance measured at a current density of 100 mA cm^{-2}. [h] Taken at 100 mA cm^{-2}.

of 100 and 1000 cd m^{-2} are 4.9 and 6.4 V, respectively. For G3 device, the turn-on voltage is 3.6 V and the maximum luminance of over 38000 cd m^{-2} is achieved at a driving voltage of 10.6 V. The maximum luminance efficiency and power efficiency are 43.13 cd A^{-1} and 21.16 lm W^{-1}, respectively. The driving voltages to get the practical brightness of 100 and 1000 cd m^{-2} are 4.4 and 5.4 V, respectively. Among all devices, G4 fabricated with complex **4** as the guest material displays the best performance. The maximum luminance for device G4 is over 39000 cd m^{-2}, and the maximum luminance efficiency and power efficiency are 50.8 cd A^{-1} and 29.0 lm W^{-1}, respectively. For both devices G3 and G4, it can be observed that the maximum luminance values can be retained during a driving voltage range, suggesting that they exceed the measurement limitation for our equipment.

As discussed, complexes **5** and **6** show weak phosphorescence in solution and the EPESS phenomenon. The maximum luminance data are 24863 and 23411 cd m^{-2} for G5 and G6, respectively. The maximum power/current efficiency values are 20.58 (lm W^{-1})/39.67 (cd A^{-1}) and 19.60 (lm W^{-1})/38.68 (cd A^{-1}), respectively.

CONCLUSION

In conclusion, five interesting bis-cyclometalated iridium complexes with tpip as the ancillary ligand have been successfully prepared and applied in the OLEDs. The tifluoromethyl substituents at different positions on the phenyl rings of ppy in iridium complexes can affect their emission color and intensity obviously. The devices ITO/TAPC (30 nm)/Ir (x wt %):SimCP2 (15 nm)/TPBi (45 nm)/LiF (1 nm)/Al (100 nm) show good performances constructed by these Ir^{3+} complexes as the emitters. For Ir^{3+} complex **4**-based device G4 where x = 8 wt %, a maximum luminance of over 39000 cd m^{-2} and a maximum luminance efficiency (η_L) and a power efficiency (η_p) of 50.8 cd A^{-1} and 29.0 lm W^{-1}, respectively, were obtained. The results suggested that all of the complexes have potential applications in OLEDs.

ASSOCIATED CONTENT

Supporting Information

X-ray crystallographic data in CIF format, selected bond lengths and angles, percent composition of the MOs and the assignment of different fragments, lifetime curves, and TGA–DSC thermal curves. This material is available free of charge via the Internet at http://pubs.acs.org.

AUTHOR INFORMATION

Corresponding Author

*Tel: 0086 25 83596775. Fax: 0086 25 83314502. E-mail: yxzheng@nju.edu.cn.

Notes

The authors declare no competing financial interest.

ACKNOWLEDGMENTS

This work was supported by the Major State Basic Research Development Program (Grants 2013CB922101 and 2011CB808704) and the National Natural Science Foundation of China (Grants 20971067 and 21021062).

REFERENCES

(1) (a) Xiao, L. X.; Chen, Z. J.; Qu, B.; Luo, J. X.; Kong, S.; Gong, Q. H.; Kido, J. J. *Adv. Mater.* **2011**, *23*, 926–952. (b) Pu, Y. J.; Iguchi, N.; Aizawa, N.; Sasabe, H.; Nakayama, K.; Kido, J. *Org. Electron.* **2011**, *12*, 2103–2110. (c) Hsieh, C. H.; Wu, F. I.; Fan, C. H.; Huang, M. J.; Lu, K. Y.; Chou, P. Y.; Yang, Y. H. O.; Wu, S. H.; Chen, I. C.; Chou, S. H.; Wong, K. T.; Cheng, C. H. *Chem.—Eur. J.* **2011**, *17*, 9180–9187. (d) Hong, Y. N.; Lam, J. W. Y.; Tang, B. Z. *Chem. Soc. Rev.* **2011**, *40*, 5361–5388. (e) Fantacci, S.; De Angelis, F. *Coord. Chem. Rev.* **2011**, *255*, 2704–2726. (f) Chou, P. T.; Chi, Y.; Chung, M. W.; Lin, C. C. *Coord. Chem. Rev.* **2011**, *255*, 2653–2665. (g) Chen, S. M.; Tan, G. P.; Wong, W. Y.; Kwok, H. S. *Adv. Funct. Mater.* **2011**, *21*, 3785–3793. (h) Chen, Z. Q.; Bian, Z. Q.; Huang, C. H. *Adv. Mater.* **2010**, *22*, 1534–1539. (i) Zhou, G. J.; Wang, Q.; Wong, W. Y.; Ma, D. G.; Wang, L. X.; Lin, Z. Y. *J. Mater. Chem.* **2009**, *19*, 1872–1883. (j) Wong, W. Y.; Ho, C. L. *J. Mater. Chem.* **2009**, *19*, 4457–4482. (k) Kim, J. J.; You, Y.; Park, Y. S.; Kim, J. J.; Park, S. Y. *J. Mater. Chem.* **2009**, *19*, 8347–8359. (l) Lo, S. C.; Bera, R. N.; Harding, R. E.; Burn, P. L.; Samuel, I. D. W. *Adv. Funct. Mater.* **2008**, *18*, 3080–3090. (m) Kang, D. M.; Kang, J. W.; Park, J. W.; Jung, S. O.; Lee, S. H.; Park, H. D.; Kim, Y. H.; Shin, S. C.; Kim, J. J.; Kwon, S. K. *Adv. Mater.* **2008**, *20*, 2003–2007. (n) Du, B.-S.; Lin, C.-H.; Chi, Y.; Hung, J.-Y.; Chung, M.-W.; Lin, T.-Y.; Lee, G.-H.; Wong, K.-T.; Chou, P.-T.; Hung, W.-Y.; Chiu, H.-C. *Inorg. Chem.* **2010**, *49*, 8713–8723. (o) Schneidenbach, D.; Ammermann, S.; Debeaux, M.; Freund, A.; Zöllner, M.; Daniliuc, C.; Jones, P. G.; Kowalsky, W.; Johannes, H.-H. *Inorg. Chem.* **2010**, *49*, 397–406. (p) Ren, X. F.; Kondakova, M. E.; Giesen, D. J.; Rajeswaran, M.; Madaras, M.; Lenhart, W. C. *Inorg. Chem.* **2010**, *49*, 1301–1303. (q) Chang, Y.-Y.; Hung, J.-Y.; Chi, Y.; Chyn, J.-P.; Chung, M.-W.; Lin, C.-L.; Chou, P.-T.; Lee, G.-H.; Chang, C.-H.; Lin, W.-C. *Inorg. Chem.* **2011**, *50*, 5075–5084. (r) Rai, V. K.; Nishiura, M.; Takimoto, M.; Zhao, S.; Liu, Y.; Hou, Z. M. *Inorg. Chem.* **2012**, *51*, 822–835. (s) Fernández-Hernández, J. M.; Yang, C.-H.; Beltrán, J. I.; Lemaur, V.; Polo, F.; Fröhlich, R.; Cornil, J.; Cola, L. D. *J. Am. Chem. Soc.* **2011**, *133*, 10543–10558.

(2) (a) Lamansky, S.; Djurovich, P.; Murphy, D.; Abdel-Razzaq, F.; Lee, H. E.; Adachi, C.; Burrow, P. E.; Forrest, S. R.; Thompson, M. E. *J. Am. Chem. Soc.* **2001**, *123*, 4304–4312. (b) Park, N. G.; Kwak, M. Y.; Kim, B. O.; Kwon, O. K.; Kim, Y. K.; You, B. R.; Kim, T. W.; Kim, Y. S. *Jpn. J. Appl. Phys.* **2002**, *41*, 1523–1526. (c) Tamayo, A. B.; Alleyne, B. D.; Djurovich, P. I.; Lamansky, S.; Tsyba, I.; Ho, N. N.; Bau, R.; Thompson, M. E. *J. Am. Chem. Soc.* **2003**, *125*, 7377–7387. (d) Tsuzuki, T.; Shirasawa, N.; Suzuki, T.; Tokito, S. *Adv. Mater.* **2003**, *15*, 1455. (e) Wong, W. Y.; Ho, C. L.; Gao, Z. Q.; Mi, B. X.; Chen, C. H.; Cheah, K. W.; Lin, Z. Y. *Angew. Chem., Int. Ed.* **2006**, *45*, 7800–

7803. (f) Tanaka, D.; Sasabe, H.; Li, Y. J.; Su, S. J.; Takeda, T.; Kido, J. *Jpn. J. Appl. Phys.* **2007**, *46*, L117−L119. (g) Chou, H. H.; Cheng, C. H. *Adv. Mater.* **2010**, *22*, 2468−2471. (h) Tao, Y. T.; Wang, Q. A.; Yang, C. L.; Zhong, C.; Qin, J. G.; Ma, D. G. *Adv. Funct. Mater.* **2010**, *20*, 2923−2929.

(3) (a) Hung, L. S.; Chen, C. H. *Mater. Sci. Eng., R* **2002**, *39*, 143−222. (b) Yang, C.-H.; Li, S.-W.; Chi, Y.; Cheng, Y.-M.; Yeh, Y.-S.; Chou, P.-T.; Lee, G.-H.; Wang, C.-H.; Shu, C.-F. *Inorg. Chem.* **2005**, *44*, 7770−7780. (c) Ragni, R.; Plummer, E. A.; Brunner, K.; Hofstraat, J. W.; Babudri, F.; Farinola, G. M.; Naso, F.; De Cola, L. *J. Mater. Chem.* **2006**, *16*, 1161−1170. (d) Dedeian, K.; Shi, J.; Forsythe, E.; Morton, D. C.; Zavalij, P. Y. *Inorg. Chem.* **2007**, *46*, 1603−1611. (e) Slinker, J. D.; Rivnay, J.; Moskowitz, J. S.; Parker, J. B.; Bernhard, S.; Abruña, H. D.; Malliaras, G. G. *J. Mater. Chem.* **2007**, *17*, 2976−2988. (f) Ho, C. L.; Wong, W. Y.; Wang, Q.; Ma, D. G.; Wang, L. X.; Lin, Z. Y. *Adv. Funct. Mater.* **2008**, *18*, 928−937. (g) Ulbricht, C.; Beyer, B.; Friebe, C.; Winter, A.; Schubert, U. S. *Adv. Mater.* **2009**, *21*, 4418−4441. (h) Sykes, D.; Tidmarsh, I. S.; Barbieri, A.; Sazanovich, I. V.; Weinstein, J. A.; Ward, M. D. *Inorg. Chem.* **2011**, *50*, 11323−11339. (i) Ladouceur, S.; Fortin, D.; Zysman-Colman, E. *Inorg. Chem.* **2011**, *50*, 11514−11526. (j) Zheng, Y.; Batsanov, A. S.; Edkins, R. M.; Beeby, A.; Bryce, M. R. *Inorg. Chem.* **2012**, *51*, 290−297. (k) Hu, T.; He, L.; Duan, L.; Qiu, Y. *J. Mater. Chem.* **2012**, *22*, 4206−4215. (l) Shavaleev, N. M.; Monti, F.; Costa, R.; Scopelliti, R.; Bolink, H.; Ortí, E.; Accorsi, G.; Armaroli, N.; Baranoff, E.; Grätzel, M.; Nazeeruddin, Md. K. *Inorg. Chem.* **2012**, *51*, 2263−2271.

(4) (a) Miller, T. M.; Neenan, T. X.; Zayas, R.; Bair, H. E. *J. Am. Chem. Soc.* **1992**, *114*, 1018−1025. (b) Bao, Z.; Lovinger, A. J.; Brown, J. *J. Am. Chem. Soc.* **1998**, *120*, 207−208. (c) Sakamoto, Y.; Suzuki, T.; Miura, A.; Fujikawa, H.; Tokito, S.; Taga, Y. *J. Am. Chem. Soc.* **2000**, *122*, 1832−1836. (d) Wang, Y.; Herron, N.; Grushin, V. V.; LeCloux, D.; Petrov, V. *Appl. Phys. Lett.* **2001**, *79*, 449−451. (e) Grushin, V. V.; Herron, N.; LeCloux, D. D.; Marshall, W. J.; Petrov, V. A.; Wang, Y. *Chem. Commun.* **2001**, 1494−1495. (f) Ionkin, A. S.; Marshall, W. J.; Roe, D. C.; Wang, Y. *Dalton Trans.* **2006**, 2468−2478. (g) Takizawa, S.-Y.; Nishida, J.-I.; Tsuzuki, T.; Tokito, S.; Yamashita, Y. *Inorg. Chem.* **2007**, *46*, 4308−4319. (h) Yang, C.-H.; Cheng, Y.-M.; Chi, Y.; Hsu, C.-J.; Fang, F.-C.; Wong, K.-T.; Chou, P.-T.; Chang, C.-H.; Tsai, M.-H.; Wu, C.-C. *Angew. Chem., Int. Ed.* **2007**, *46*, 2418−2421. (i) Babudri, F.; Farinola, G. M.; Naso, F.; Ragni, R. *Chem. Commun.* **2007**, 1003−1022. (j) Chou, P.-T.; Chi, Y. *Chem.—Eur. J.* **2007**, *13*, 380−395. (k) Chiu, Y.-C.; Hung, J.-Y.; Chi, Y.; Chen, C.-C.; Chang, C.-H.; Wu, C.-C.; Cheng, Y.-M.; Yu, Y.-C.; Lee, G.-H.; Chou, P.-T. *Adv. Mater.* **2009**, *21*, 2221−2225.

(5) (a) Lee, S.-C.; Kim, Y. S. *Mol. Cryst. Liq. Cryst.* **2008**, *491*, 209−216. (b) Coppo, P.; Plummer, E. A.; De Cola, L. *Chem. Commun.* **2004**, 1774−1775.

(6) (a) You, Y.; Park, S. Y. *J. Am. Chem. Soc.* **2005**, *127*, 12438−12439. (b) Li, J.; Djurovich, P. I.; Alleyne, B. D.; Tsyba, I.; Ho, N. N.; Bau, R.; Thompson, M. E. *Polyhedron* **2004**, *23*, 419−428. (c) Lamansky, S.; Djurovich, P.; Murphy, D.; Abdel-Razzaq, F.; Kwong, R.; Tsyba, I.; Bortz, M.; Mui, B.; Bau, R.; Thompson, M. E. *Inorg. Chem.* **2001**, *40*, 1704−1711. (d) Kwon, T.-H.; Cho, H. S.; Kim, M. K.; Kim, J.-W.; Kim, J.-J.; Lee, K. H.; Park, S. J.; Shin, I.-S.; Kim, H.; Shin, D. M.; Chung, Y. K.; Hong, J.-I. *Organometallics* **2005**, *24*, 1578−1585.

(7) (a) Zhu, Y. C.; Zhou, L.; Li, H. Y.; Xu, Q. L.; Teng, M. Y.; Zheng, Y. X.; Zuo, J. L.; Zhang, H. J.; You, X. Z. *Adv. Mater.* **2011**, *23*, 4041−4046. (b) Teng, M. Y.; Zhang, S.; Jiang, S. W.; Yang, X.; Lin, C.; Zheng, Y. X.; Wang, L. Y.; Wu, D.; Zuo, J. L.; You, X. Z. *Appl. Phys. Lett.* **2012**, *100*, 073303−073306.

(8) Rillema, D. P.; Taghdiri, D. G.; Jones, D. S.; Keller, C. D.; Worl, L. A.; Meyer, T. J.; Levy, H. A. *Inorg. Chem.* **1987**, *26*, 578−585.

(9) King, K. A.; Spellane, P. J.; Watts, R. J. *J. Am. Chem. Soc.* **1985**, *107*, 1431−1432.

(10) (a) Lee, C. T.; Yang, W. T.; Parr, R. G. *Phys. Rev. B* **1988**, *37*, 785−789. (b) Del Bene, J. E.; Person, W. B.; Szczepaniak, K. *J. Phys. Chem.* **1995**, *99*, 10705−10707. (c) Chiodo, S.; Russo, N.; Sicilia, E. *J. Chem. Phys.* **2006**, *125*, 104107. (d) Cossi, M.; Scalmani, G.; Rega, N.; Barone, V. *J. Comput. Chem.* **2003**, *24*, 669−681. (e) Frisch, M. J.; Trucks, G. W.; Schlegel, H. B.; Scuseria, G. E.; Robb, M. A.; Cheeseman, J. R.; Scalmani, G.; Barone, V.; Mennucci, B.; Petersson, G. A.; Nakatsuji, H.; Caricato, M.; Li, X.; Hratchian, H. P.; Izmaylov, A. F.; Bloino, J.; Zheng, G.; Sonnenberg, J. L.; Hada, M.; Ehara, M.; Toyota, K.; Fukuda, R.; Hasegawa, J.; Ishida, M.; Nakajima, T.; Honda, Y.; Kitao, O.; Nakai, H.; Vreven, T.; Montgomery, J. A., Jr.; Peralta, J. E.; Ogliaro, F.; Bearpark, M.; Heyd, J. J.; Brothers, E.; Kudin, K. N.; Staroverov, V. N.; Kobayashi, R.; Normand, J.; Raghavachari, K.; Rendell, A.; Burant, J. C.; Iyengar, S. S.; Tomasi, J.; Cossi, M.; Rega, N.; Millam, J. M.; Klene, M.; Knox, J. E.; Cross, J. B.; Bakken, V.; Adamo, C.; Jaramillo, J.; Gomperts, R.; Stratmann, R. E.; Yazyev, O.; Austin, A. J.; Cammi, R.; Pomelli, C.; Ochterski, J. W.; Martin, R. L.; Morokuma, K.; Zakrzewski, V. G.; Voth, G. A.; Salvador, P.; Dannenberg, J. J.; Dapprich, S.; Daniels, A. D.; Farkas, O.; Foresman, J. B.; Ortiz, J. V.; Cioslowski, J.; Fox, D. J. *Gaussian 09*, revision A.01; Gaussian, Inc.: Wallingford, CT, 2009.

(11) *SAINT-Plus*, version 6.02; Bruker Analytical X-ray System: Madison, WI, 1999.

(12) Sheldrick, G. M. *SADABS: An empirical absorption correction program*; Bruker Analytical X-ray Systems: Madison, WI, 1996.

(13) (a) Sheldrick, G. M. *SHELXTL-97*; Universität Göttingen: Göttingen, Germany, 1997. (b) Farrugia, L. J. *J. Appl. Crystallogr.* **1997**, *30*, 565.

(14) Magennis, S. W.; Parsons, S.; Pikramenou, Z. *Chem.—Eur. J.* **2002**, *8*, 5761−5771.

(15) Nonoyama, M. *J. Organomet. Chem.* **1975**, *86*, 263−267.

(16) Lee, S. J.; Park, K. M.; Yang, K.; Kang, Y. J. *Inorg. Chem.* **2009**, *48*, 1030−1037.

(17) (a) Spellane, P.; Watts, R. J.; Vogler, A. *Inorg. Chem.* **1993**, *32*, 5633−5636. (b) Tsuboyama, A.; Iwawaki, H.; Furugori, M.; Mukaide, T.; Kamatani, J.; Igawa, S.; Moriyama, T.; Miura, S.; Takiguchi, T.; Okada, S.; Hoshino, M.; Ueno, K. *J. Am. Chem. Soc.* **2003**, *125*, 12971−12979.

(18) (a) Cummings, S. D.; Eisenberg, R. *J. Am. Chem. Soc.* **1996**, *118*, 1949−1960. (b) Lees, A. J. *Comments. Inorg. Chem.* **1995**, *17*, 319−346.

(19) (a) Baldo, M. A.; Adachi, C.; Forrest, S. R. *Phys. Rev. B* **2000**, *62*, 10967−10977. (b) Namdas, E. B.; Ruseckas, A.; Samuel, D. W.; Lo, S. C.; Burn, P. L. *Appl. Phys. Lett.* **2005**, *86*, 091104−091106.

(20) (a) Zhao, Q.; Li, L.; Li, F. Y.; Yu, M. X.; Liu, Z. P.; Yi, T.; Huang, C. H. *Chem. Commun.* **2008**, 685−687. (b) You, Y.; Huh, H. S.; Kim, K. S.; Lee, S. W.; Kim, D.; Park, S. Y. *Chem. Commun.* **2008**, 3998−4000. (c) Shin, C. H.; Huh, J. O.; Lee, M. H.; Do, Y. *Dalton Trans.* **2009**, 6476−6479. (d) Shin, C. H.; Huh, J. O.; Lee, M. H.; Do, Y. *Eur. J. Inorg. Chem.* **2010**, 3642−3651. (e) Wu, H. Z.; Yang, T.; Zhao, S, Q.; Zhou, J.; Li, C. Y.; Li, F. Y. *Dalton Trans.* **2011**, *40*, 1969−1976.

(21) (a) Bettington, S.; Tavasli, M.; Bryce, M. R.; Beeby, A.; Al-Attar, H.; Monkman, A. P. *Chem.—Eur. J.* **2007**, *13*, 1423−1428. (b) Nazeeruddin, M. K.; Wegh, R. T.; Zhou, Z.; Klein, C.; Wang, Q.; Angelis, F. D.; Fantacci, S.; Grätzel, M. *Inorg. Chem.* **2006**, *45*, 9245−9250.

(22) (a) Ashraf, R. S.; Shahid, M.; Klemm, E.; Al-Ibrahim, M.; Sensfuss, S. *Macromol. Rapid Commun.* **2006**, *27*, 1454−1459. (b) Thelakkat, M.; Schmidt, H. W. *Adv. Mater.* **1998**, *10*, 219−223.